ATEMA' 2007
Montréal
August 6 - 10, 2007

International Conference on Advances and Trends in Engineering Materials and their Applications (AES – ATEMA' 2007)

2D Phase-Field Simulation of Static Recrystallization

K. Tanaka[1]*, T. Takaki[2], Y. Tomita[3]

[1] *Graduate School of Science and Technology, Kobe University, 1-1, Rokkodai, Nada, Kobe 657-8501, Japan

(Email:tanaka@solid.mech.kobe-u.ac.jp)

[2] Faculty of Maritime Sciences, Kobe University, 5-1-1, Fukaeminami, Higashinada, Kobe, 658-0022, Japan

(Email: takaki@maritime.kobe-u.ac.jp)

[3] Faculty of Engineering, Kobe University, 1-1, Rokkodai, Nada, Kobe 657-8501, Japan

(Email: tomita@mech.kobe-u.ac.jp)

*Corresponding Author

Abstract

In this study, we have performed a series of numerical simulations of the static recrystallization process using the numerical model developed in our previous study. The numerical model enables us to continuously simulate the process from the deformation of a polycrystal metal to the annealing by coupling the crystal plasticity finite element method and the phase-field method. The simulations were carried out under the conditions of two different grain sizes and two different nucleation models, i.e., site saturated nucleation and continuous-nucleation rate models. As a result, the numerical results for different grain sizes indicate that the size fluctuation of recrystallized grains is larger and the

recrystallization kinetics is slower for the polycrystal with large grains than that with small grains. These phenomena were reproduced by introducing strain-gradient theory into the crystal plasticity finite element method to simulate the size-dependent work hardening. Furthermore, we point out the importance of the nucleation model and the possibility of the development of a novel numerical model taking the spontaneous nucleation formed during recovery into account.

Keywords
Static Recrystallization, Phase-Field Method, Crystal Plasticity, Nucleation, Recovery.

1 Introduction

The establishment of a numerical model and simulation technique will enable us to obtain the optimum design and perform precise predictions of material microstructures formed during annealing [1]. Therefore, much effort has been devoted to developing numerical models of recrystallization [2], and various phenomena have been investigated from the viewpoints of numerical simulations [3, 4].

It is widely recognized that the microstructures formed during annealing are significantly affected by the pre-deformation microstructures [5], since the recrystallization originates from dislocation cells or subgrains that appear after deformation, and subsequently, the recrystallized grain growth is driven by the stored energy resulting from the dislocation accumulated during deformation. Recently, numerical studies using the Monte Carlo (MC) Potts model [6] and the cellular automata (CA) model [7] based on the data measured by electron back-scatter diffraction (EBSD) analyses have been performed for static recrystallization. However, to enable more systematic investigations of recrystallization textures, it is essential to develop a computational procedure that does not use experimental data.

In this study, we perform a series of numerical simulations of the static recrystallization process. The effects of the grain size and the nucleation model on the recrystallization microstructure and kinetics are investigated. Here, we employ the coupled numerical model developed in Ref. [8], in which the deformation of polycrystalline metal is simulated using the finite element (FE) method based on strain-gradient crystal plasticity theory, and the nucleation and growth of the recrystallized

206

grains are simulated by the phase-field method.

2 Numerical Procedure

In this study, we employ the numerical procedure for static recrystallization proposed by Takaki et al. [8]. Figure 1 shows the computational sequence composed of the following three steps: the deformation simulation, the data mapping and the recrystallization simulation. Next, we briefly explain each step.
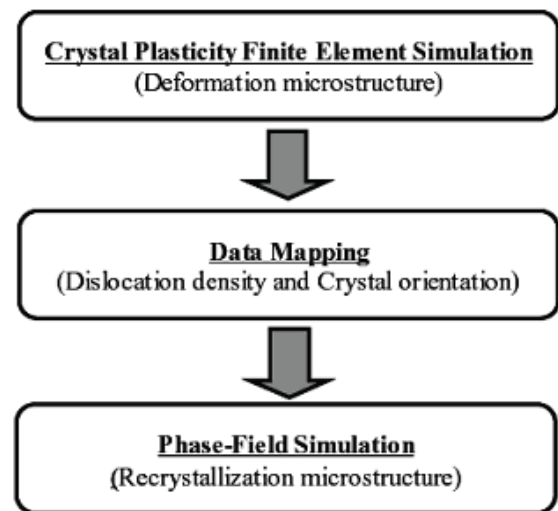

Figure 1. Numerical procedure.

2.1 Crystal plasticity FE simulation

The crystal plasticity FE method based on the strain-gradient theory of rate-dependent plasticity [9] is used to examine the microstructure and dislocation distribution during the deformation of polycrystalline metals. Here, the critical resolved shear stress $g^{(a)}$ on slip system (a) is assumed to be expressed by a Bailey-Hirsch function:

$$g^{(a)} = g_0^{(a)} + a\mu b \sum_{(b)} \omega_{ab} \sqrt{\rho^{(b)}} , \qquad (1)$$

where $g_0^{(a)}$ is the initial value of $g^{(a)}$, a is a

constant, μ is the elastic shear modulus, b is the magnitude of the Burgers vector, ω_{ab} is the interaction matrix and $\rho^{(b)}$ is the accumulated dislocation density, which is the sum of the densities of the statistically stored dislocations (SSDs) and the geometrically necessity dislocations (GNDs). The evolution of the SSDs is expressed by the balance between the production rate of dislocations and the annihilation by dynamic recovery. The density of the GNDs is calculated from the gradient of the shear strain on slip system (a). Since the hardening equation, Eq. 1, includes the strain-gradient term through the dislocation density, it is possible to express the effects of the grain size.

2.2 Data mapping

The data calculated by the crystal plasticity FE simulation, such as the dislocation density and crystal orientation, are mapped onto a regular lattice used in the phase-field simulation. The stored energies calculated from the dislocation density are smoothed on the lattice, because the phase-field method requires spatially continuous driving forces.

2.3 Phase-field simulation

We generalize the phase-field model proposed by Kobayashi, Warren and Carter, i.e., KWC model [9,10,11] to simulate the migration of the recrystallized grain boundary driven by the stored energy and the impingement between the recrystallized grains. In this model, two order parameters, phase field ϕ and crystallographic orientation θ, are used. The time evolution equations for ϕ and θ are as follows:

$$\frac{\partial \phi}{\partial t} = M_\phi \left[\alpha^2 \nabla^2 \phi - \frac{\partial f(\phi)}{\partial \phi} - 2\phi s |\nabla \theta| \right] \qquad (2)$$

$$\frac{\partial \theta}{\partial t} = M_\theta \frac{1}{\phi^2} \nabla \cdot \left(\phi^2 s \frac{\nabla \theta}{|\nabla \theta|} \right), \qquad (3)$$

where α is the gradient coefficient, s is a constant, M_ϕ is the mobility of ϕ and M_θ is the mobility of θ. The parameters are selected as $\alpha = (3\delta\sigma)^{0.5}$, $s = \alpha(2W)^{0.5}/\pi$, $M_\phi = m(2W)^{0.5}/6\alpha$ and $M_\theta = (1-p(\phi))M_\phi$, where σ is the interface energy, δ is the interface thickness and m is the mobility of the grain boundary migration. The free energy density $f(\phi)$ is expressed by following double-well function:

$$f(\phi) = (1 - p(\phi))E_{store} + Wq(\phi). \qquad (4)$$

Here, $p(\phi) = \phi^3(10-15\phi+6\phi^2)$ and $q(\phi)=\phi^2(1-\phi)^2$. E_{store} is the stored energy calculated by $E_{store} = 0.5\rho\mu b^2$, where ρ is the dislocation density. W is the barrier height expressed by $W = 6\sigma/\delta$.

3 Simulation Results
3.1 Deformation simulation

Figure 2 shows the polycrystal model consisting of 23 regular grains. This model is divided into 64x64 regular crossed-triangle elements and is compressed at a strain rate 10^{-3} [1/s] as a 2-slip plane-strain problem. Figures 3 (a) and (b) illustrate the numerical results of the crystallographic orientation at a compression of 50% thickness for 23-and 77-grain models, respectively. From Fig. 3, we can observe the misorientation inside some of the original grains.

The dislocation densities and crystal orientations are utilized as basic data in the static recrystallization simulation using the phase-field method.
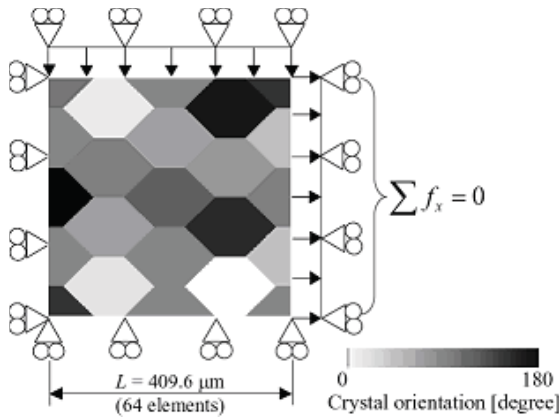
207

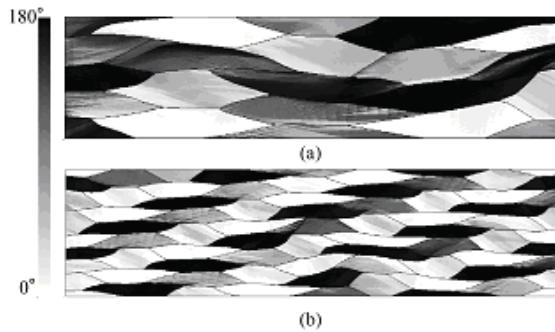*Figure 2.* Polycrystal computational model with 23 regular grains.

Figure 3. Crystallographic orientation at 50% compression for (a) 23-grain model and (b) 77-grain model.

3.2 Static recrystallization simulation

The nucleation and growth of recrystallized grains during annealing are simulated by the phase-field method based on the data calculated by the crystal plasticity FE simulation. Although the grain boundary migration of the recrystallized grains follows Eqs. 2 and 3, the nucleation of the recrystallization is not defined yet. It is the most difficult process to simulate because of the difficulty of its experimental observation. Although there are still uncertainties about nucleation mechanisms, some points have been clarified [5]. On the basis of the points and the

208

conditions that must be considered from a computational viewpoint, the following criteria are defined: (1) a high-angle grain boundary of more than 15 degrees, (2) a stored energy of more than 0.6 MPa, (3) the orientation of the nucleus is present in the deformed structure and (4) the minimum distance between two neighboring nuclei is 10 Δx, where Δx is the grid size. The initial radius of the nucleus is set to 3 Δx. Here, we choose the following material parameters: $\Delta x = 0.4$ [μm], $\delta = 0.8$ [μm], $dt = 0.1$ [s], $\sigma = 0.6$ [J/m^2], $\alpha = 1.14 \times 10^{-3}$ [(J/m)$^{0.5}$], $m = 4.11 \times 10^{-14}$ [m^3/Ns], $W = 4.94 \times 10^6$ [J/m^3] and $M_\phi = 1.8 \times 10^{-8}$ [m^3/Js].

Next, we consider two types of nucleation models, one is the site saturated nucleation (SSN) model and the other is the constant-nucleation-rate (CNR) model. In the CNR model, we consider the nucleation rate to be $\dot{N}(1-X)$, where $\dot{N}$ is the constant nucleation rate and X is the recrystallized volume fraction. This means that the nucleation rate gradually decreases with recrystallization [5, 12].

Figure 4 shows the initial nucleation sites of (a) 23-grain and (b) 77-grain models using SSN. It is observed that there are many nuclei around the original and newly developed grain boundaries; thus, is confirmed that nucleation can occur on the basis of the defined nucleation criteria. It is widely recognized from experimental observations that the grain boundaries and the misoriented transition bands inside the grains are active nucleation sites [5, 12].
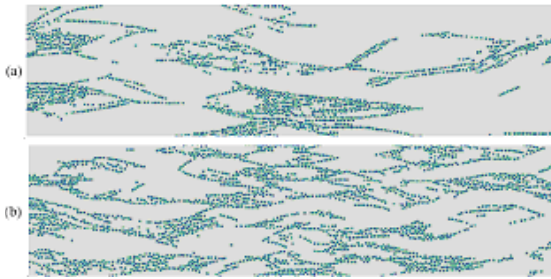
Figure 4. Initial nucleation sites of (a) 23-grain model and (b) 77-grain model.

Figures 5 and 6 illustrate the recrystallized grain growth process of the 23-grain model using SSN and CNR, respectively. The white region indicates the deformed material and the grain boundary between recrystallized grains, and the black region shows the recrystallized grains. From Fig. 6, we can observe continuous nucleation during the recrystallization.

Figure 7 shows the final recrystallized microstructures. Comparing the 23-and 77-grain models, it is observed that the size fluctuation of the recrystallized grains is larger for the 23-grain model than the 77-grain one.
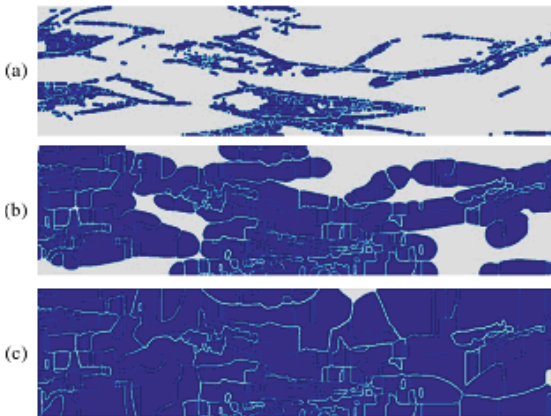

Figure 5. Recrystallized microstructure evolution for 23-grain model using SNR. $t =$ (a) 100, (b) 1000 and (c) 3000 s.
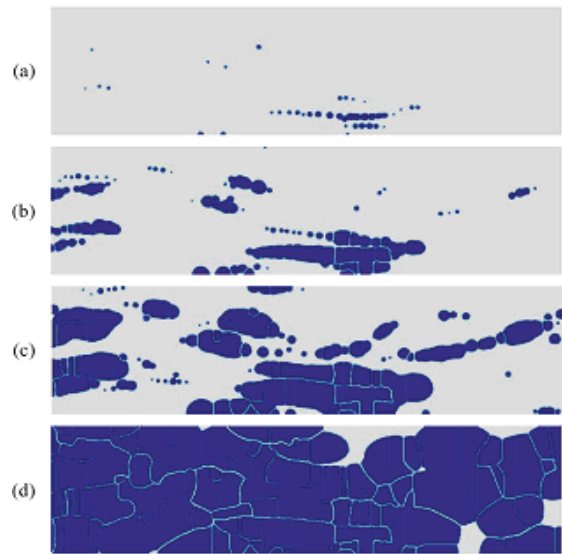

Figure 6. Recrystallized microstructure evolution for 23-grain model using CNR. $t =$ (a) 100, (b) 500, (c) 1000 and (d) 3000 s.

This fluctuation depends on the distribution of the nucleation sites, as shown in Fig. 4. Since the nucleation sites are determined from the deformed microstructures, it is confirmed that the recrystallized microstructures are largely dependent on their location. Furthermore, from Fig. 7, we can see the recrystallized grains with the characteristic shape elongated in the vertical direction.
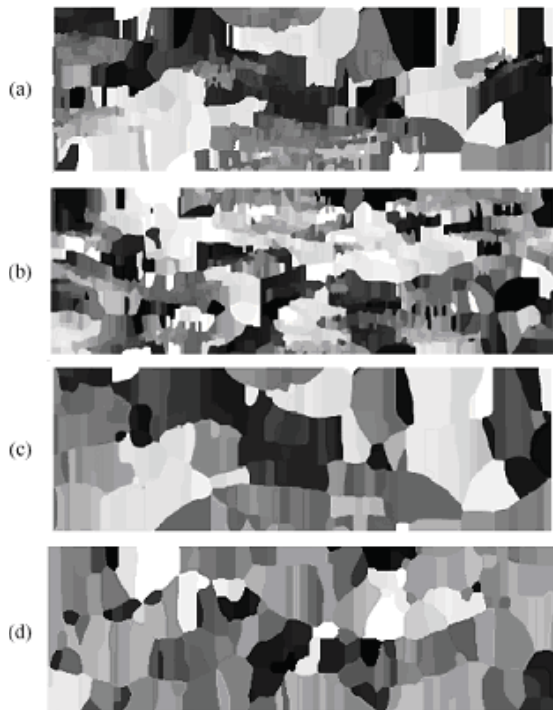
Figure 8 illustrates the variation of the

Figure 7. Final recrystallized microstructures of (a) 23-grain model using SSN, (b) 77-grain model using SSN, (c) 23-grain model using CNR and (d) 77-grain model using CNR.

recrystallization volume fraction. From Fig. 8, it can be seen that the recrystallization rate of the 77-grain model is faster than that of the 23-grain model for both nucleation models. This tendency is identical with the reported experimental result that the recrystallization rate of large pregrains is slower than that of small pregrains [5]. This is because that the stored energy inside grains is higher for small pregrains than large ones, and by introducing strain-gradient theory to crystal plasticity, this phenomena can be reproduced. In the CNR model, the typical S-shaped curves can be observed for both 23-and 77-grain models. Figure 9 shows the Jhonson, Mehl, Avrami and Kolmogorov (JMAK) plots corresponding to Fig. 8 [5]. The JMAK plot characterizes the

210

recrystallization kinetics, and its gradient is known as the Avrami exponent. The theoretical values of the Avrami exponent in 2D are 2 and
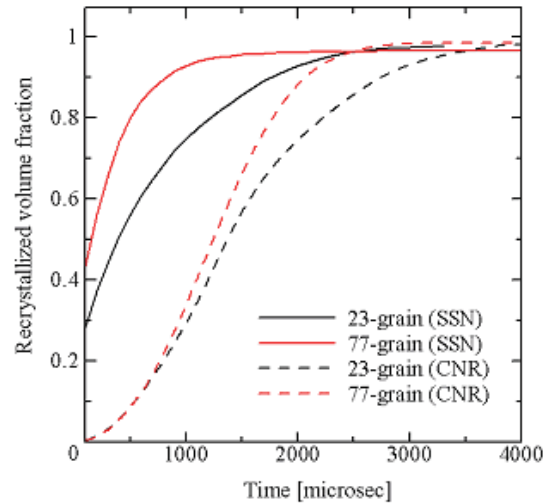

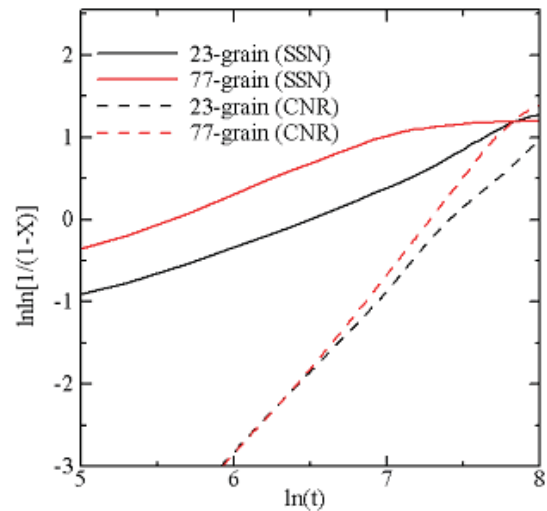*Figure 8.* Recrystallization volume fraction.

Figure 9. JMAK plots.

3 for SSN and CNR, respectively. However, as shown in Fig. 9, our calculations indicate markedly lower values than those of the theory (the Avrami exponents for the 23 grain (SSN), 77 grain (SSR), 23 grain (CNR) and 77 grain (CNR) models are 0.8, 1.0, 2.0 and 2.3, respectively). This difference is due to the

random-nucleation assumption in the theoretical calculation. In fact, it has been reported that the values of the Avrami exponent obtained from experiments are lower than those based on theory [5].

4 Discussion

As mentioned above, the simulated recrystallized microstructures are largely affected by the definition of the nucleation model. Therefore, the development of a precise nucleation model based on the actual nucleation mechanism will be indispensable. Although abnormal grain growth is recognized as one of the possible nucleation mechanisms and is reproduced by MC and CA simulations, the effects of the rotation of grains or their coalescence during recovery on the recrystallization nucleation is still hardly understood. The KWC phase-field model employed in this study can simulate the grain boundary migration and the grain rotation simultaneously. Therefore, we believe that, by generalizing the numerical procedure used in this study, we will be able to construct a static recrystallization model of spontaneous nucleation including both abnormal grain growth and coalescence and taking the deformation microstructure into account.

5 Conclusions

In this study, we have performed a series of numerical simulations of static recrystallization, in which the numerical model coupled with the crystal plasticity finite element method and the phase-field method was employed. The numerical results for different grain sizes indicate that the size fluctuation of recrystallized grains is larger and the recrystallization kinetics is slower for the polycrystal with large grains than that with small grains. These tendencies are similar to the reported experiment results. Our results were obtained by introducing strain-gradient theory into the crystal plasticity finite element method to simulate size-dependent work hardening. Therefore, we anticipate the practical application of the proposed numerical procedure to the optimum design of material microstructures by the integrated evaluation from plastic deformation to annealing. In order to improve the simulation accuracy, it will be indispensable to establish a numerical model including the spontaneous nucleation. We leave this as a future work.

Acknowledgments

References

[1] Raabe, D., Hntcherli, L. (2002) Cellular automata in materials science with particular reference to recrystallization simulation, *Computational Materials Science*, 32, 53-76.

[2] Rios, P.R., Siciliano, Jr.F., Sandim, H.R.Z., Plaut, R.L., Padilha, A.F., (2005) Nucleation and growth during recrystallization, *Materials Research*., 8, 225-238.

[3] Simmons, J.P., Wen, Y., Shen, C., Wang, Y.Z. (2004) Microstructural development involving nucleation and growth phenomena simulated with Phase Field method, *Materials Science and Engineering,* A365, 136-143.

[4] Humphreys, F.J. (1992) Modelling

211

mechanisms and microstructures of recrystallization, *Materials Science and Technology*, 8, 135.

[5] Humphreys, F.J., Heatherly, M. (2004), *Recrystallization and related annealing phenomena,* Elsevier (Springer).

[6] Choi, S., Cho, J.H. (2005) Primary recrystallization modeling for interstitial free steels, *Materials Science and Engineering.,* A405, 86.

[7] Hesselbarth, H.W., Gobel, I.R. (1991) Simulation of recrystallization by cellular automata, *Acta Metallurgica et Materialia.*, 39, 2135.

[8] Takaki, T., Yamanaka, A., Higa, Y., Tomita, Y. (2007) Phase-field simulation during static recrystallization based on crystal plasticity theory, *J. Computer-Aided Material Design*, (in press).

[9] Higa, Y., Tomita, Y., Sawada, Y. (2003) Computational simulation of characteristic length dependent deformation behavior, *Trans.JSME*, A69, 523-529.

[10] Warren, J.A., Kobayashi, R., Lobkovsky, A.E., Carter, W.C. (2003) Extending phase field models of solidification to polycrystalline materials, *Acta materialia.*, 51, 6035-6058.

[11] Lobkovsky, A.E., Warren, J.A. (2001) Sharp interface limit of phase-field model of crystal grains, *Physycal Review E*, 63, 051605.

[12]Doherty, R. D., Hughes, D.A., Humphreys, F.J., Jonas, J.J., Jensen, D.J., Kassner, M.E., King, W.E., McNelley, T.R., McQueen, H.J., Rollett, A.D. (1997) Current issues in recrystallization: a review, *Materials Science and Engineering.*, A238, 219-274.

[13] Upmanyu, M., Srolovitz, D.J., Lobkovsky, A.E., Warren, J.A., Carter, W.C. (2006) Simultaneous grain boundary migration and grain rotation, *Acta Materialia*, 54, 1707-1719.

[14] Kobayashi, R., Warren, J.A., Carter, W.C. (2000) A continuum model of grain boundaries, *Physica D*, 140, 141-150.

[15] Kobayashi, R., Warren, J.A., Carter, W.C. (2000) Grain boundary model and singular diffusivity, *Mathematical Sciences and Applications*, 14, 283-294.

[16] Read, W.T., Shockley, W. (1950) Dislocation Models of Crystal Grain Boundaries*, Physics Review*, 78, 275.

212